

## Oxygen Diffusion in Pure and Doped ZnO

Antônio Claret Soares Sabioni<sup>a\*</sup>, Marcelo José Ferreira Ramos<sup>a</sup>, Wilmar Barbosa Ferraz<sup>b</sup>

<sup>a</sup>Laboratório de Difusão em Materiais, Departamento de Física,  
Universidade Federal de Ouro Preto, 35400-000 Ouro Preto - MG, Brazil

<sup>b</sup>Centro de Desenvolvimento da Tecnologia Nuclear - CDTN/CNEN,  
Pampulha, Belo Horizonte - MG, Brazil

Received: November 11, 2001; Revised: March 24, 2003

Oxygen diffusion coefficients in pure and doped ZnO polycrystals were determined by means of the gas-solid isotope exchange method using the isotope  $^{18}\text{O}$  as oxygen tracer. The diffusion experiments were performed from 900 to 1000 °C, under an oxygen pressure of  $10^5$  Pa. After the diffusion annealings, the  $^{18}\text{O}$  diffusion profiles were determined by secondary ion mass spectrometry. The results of the experiments show that oxygen diffusion in Li-doped ZnO is similar to the oxygen diffusion in pure ZnO, while in Al-doped ZnO the oxygen diffusion is enhanced in relation to that observed in pure ZnO, in the same experimental conditions. Based on these results is proposed an interstitial mechanism for oxygen diffusion in ZnO. Moreover, it was found that oxygen grain-boundary diffusion is ca. 3 to 4 orders of magnitude greater than oxygen volume diffusion in pure and doped ZnO, which means that the grain-boundary is a fast path for oxygen diffusion in ZnO.

**Keywords:** oxygen diffusion, zinc oxide, point defects, varistor

### 1. Introduction

The study of non-linear current-voltage characteristics of ZnO based varistors, as well as of its degradation in service, is of great technological importance<sup>1,2</sup>. The understanding and modelling of these phenomena need the knowledge of the defect structure in ZnO. However, the defect chemistry in ZnO is not well established yet.

An important way to characterize the defect structure in materials is by means of diffusion experiments. A number of works about oxygen diffusion in ZnO have been performed to determine the major point defect on the oxygen sublattice, but these early studies<sup>3-8</sup> show poor agreement about the point defect responsible for the oxygen diffusion in ZnO. These previous works have been reviewed in Refs.7,8.

If we take into account, for example, the two more recent works undertaken by Haneda *et al.*<sup>7</sup>, and by Tomlins *et al.*<sup>8</sup>, using modern techniques, they show total disagreement with regard to the oxygen diffusion mechanism.

Haneda *et al.*<sup>7</sup> working with polycrystals of pure ZnO, and ZnO doped with Li (3000 ppm) and with Al (3000 ppm), between 950 and 1052 °C, at an oxygen pressure of  $5 \times 10^3$  Pa, have proposed an interstitial mechanism.

On the other hand, Tomlins *et al.*<sup>8</sup> have proposed a vacancy mechanism for oxygen diffusion in ZnO, taken into account experimental results on oxygen diffusion, measured on undoped ZnO single crystalline samples, between 850 and 1200 °C, at an oxygen partial pressure of  $10^5$  Pa.

In order to elucidate the diffusion mechanism for oxygen diffusion in ZnO, a few diffusion experiments have been performed in high density polycrystals of pure and doped ZnO. The doped samples had the same aliovalent cations (Li and Al) used by Haneda *et al.*<sup>7</sup>, but with different impurity contents (500 ppm), and the diffusion experiments were performed at a different oxygen pressure ( $10^5$  Pa).

The oxygen diffusion experiments were performed using the stable isotope  $^{18}\text{O}$  as oxygen tracer, and secondary ion mass spectrometry (SIMS) to analyse the diffusion profiles.

\*e-mail: sabioni@iceb.ufop.br

Trabalho apresentado no I Simpósio Mineiro de Ciências dos Materiais, Ouro Preto, Novembro de 2001.

## 2. Experimental Procedure

### 2.1 Material

The ZnO samples were fabricated by using high-purity powder obtained from *Alfa Aesar*. The impurity content of the powder was less than 10 ppm (elements detected: Fe 0.1 ppm and Pb 1 ppm). The powder was cold pressed and sintering at 1393 °C, for 2 h in oxygen atmosphere. The ZnO samples doped with Li<sub>2</sub>O (Li 500 ppm) and Al<sub>2</sub>O<sub>3</sub> (Al 500 ppm) were also fabricated in the same conditions of the pure ZnO. No additive was used as powder agglomerant in the sintering experiments.

The sintered polycrystals of pure ZnO and Al-doped ZnO had high density (> 99 % of the value of the theoretical density). The sintered Li-doped ZnO shown an heterogenous microstructure, with dense and porous regions. In this case, the porous region was removed, and it was only used the dense part of the sample. Grain sizes were about 20 μm for pure ZnO and Al-doped ZnO and about 30 nm for Li-doped ZnO.

### 2.2 Diffusion experiments

The diffusion specimens were cut with the dimensions 1 mm × 3 mm × 3 mm, polished with diamond paste, and submitted to a pre-annealing in order to equilibrate the samples with the temperature and atmosphere to be used in the diffusion annealings.

Oxygen diffusion experiments were performed by means of the gas-solid isotopic exchange method<sup>9</sup>, using the isotope <sup>18</sup>O as oxygen tracer.

The diffusion annealings were performed at 900, 950 and 1000 °C, in an oxygen partial pressure of 10<sup>5</sup> Pa, for the pure ZnO. The doped samples were treated at 900 and 1000 °C, in the same oxygen pressure. The experimental arrangement used in these diffusion experiments is shown in Fig. 1.

### 2.3 Depth profiling by secondary ion mass spectrometry (SIMS)

The oxygen diffusion profiles were determined by SIMS using a CAMECA apparatus at Laboratoire de Physique des Solides – CNRS/Meudon-Bellevue, France.

The SIMS analysis of the oxygen isotopes were established using a 10 keV Cs<sup>+</sup> ion source. The diffusion profiles of the isotope <sup>18</sup>O was determined from the signals of the negative secondary ions <sup>16</sup>O<sup>-</sup> and <sup>18</sup>O<sup>-</sup> using the expression:

$$C = \frac{I(^{18}\text{O}^-)}{I(^{18}\text{O}^-) + I(^{16}\text{O}^-)} \quad (1)$$

The penetration depths were determined assuming a constant sputtering rate and measuring the depths of the craters by means of a profilometer Tencor.

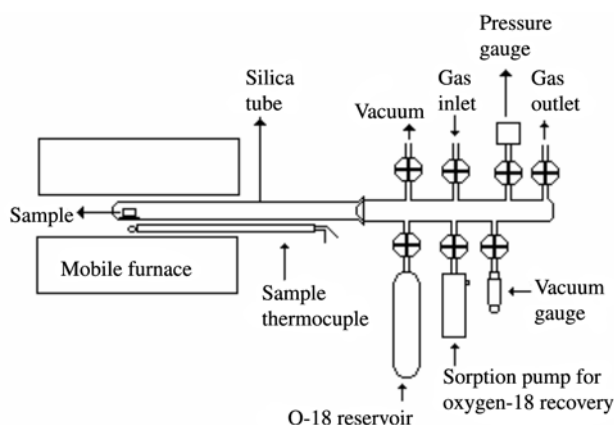


**Figure 1.** Schematic diagram of the heat treatment arrangement used for diffusion experiments by the isotope exchange method.

## 3. Results and Discussions

### 3.1 Volume diffusion in pure and doped ZnO

Figure 2 shows a diffusion profile of <sup>18</sup>O in pure ZnO, after diffusion at 900 °C, for 49 h, in an oxygen pressure of 10<sup>5</sup> Pa. The profile clearly shows two different diffusion mechanisms. The first part of the profile corresponds to the volume diffusion and the second part of profile, i.e., the tail of the profile, is a characteristic of the diffusion along the grain-boundaries<sup>9</sup>.

The volume diffusion coefficients were determined through a solution of the diffusion equation, for diffusion in a semi-infinite medium from a constant surface concentration. This solution is given by Ref. 9:

$$\frac{C_s - C(x)}{C_s - C_0} = \text{erf}\left(\frac{x}{2\sqrt{Dt}}\right) \quad (2)$$

where  $C_s$  is the concentration of the tracer at the surface,  $C(x)$  is the concentration as a function of position,  $C_0$  is the natural abundance of tracer in the ZnO (0.204%),  $x$  is the depth,  $D$  is the volume diffusion coefficient,  $t$  is the annealing time, and erf is the error function.

The volume diffusion coefficient was determined by the fit of Eq. 2 to the part of the profile concerning the volume diffusion, as shown in Fig. 2. The same procedure was used to determine the volume diffusion coefficients in doped ZnO.

Figure 3 shows the Arrhenius plot for the oxygen volume diffusion coefficients determined in pure and doped ZnO. These results show that, in the experimental conditions used in this work, oxygen diffusion in Li-doped ZnO is similar to oxygen diffusion in undoped ZnO, whilst the oxygen diffusion in Al-doped ZnO is greater than in pure ZnO.

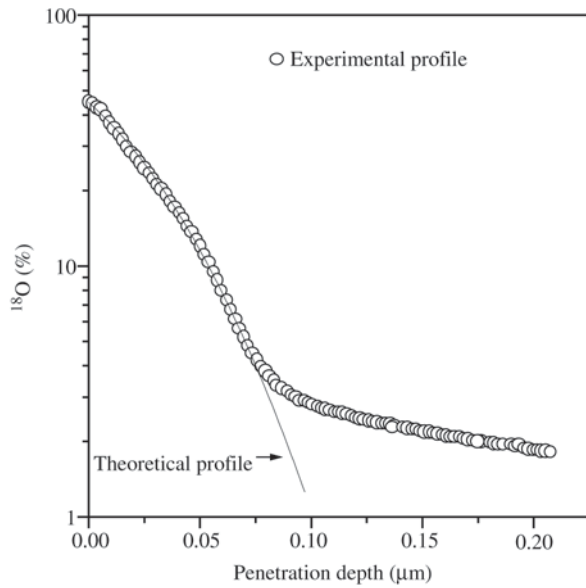


**Figure 2.** Concentration profile of  $^{18}\text{O}$  in pure ZnO polycrystal after diffusion at  $900\text{ }^\circ\text{C}$ .

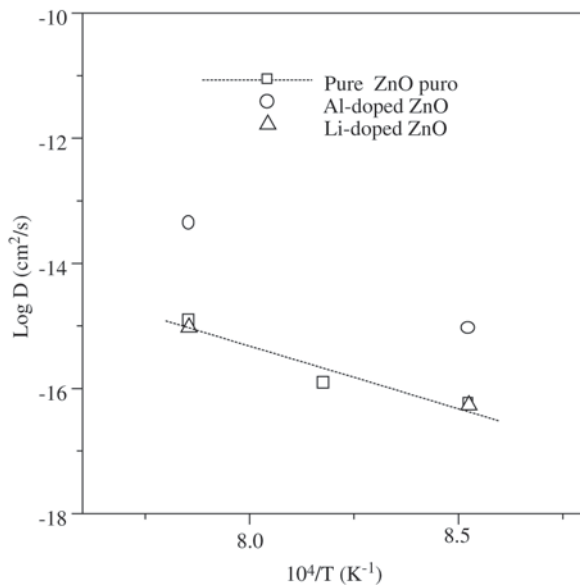


**Figure 3.** Arrhenius plot for  $^{18}\text{O}$  in pure ZnO, Li-doped ZnO and Al-doped ZnO.

### 3.2 Grain-boundary diffusion in pure and doped ZnO

The kinetics of the grain-boundary diffusion, in our experimental conditions, is of B-type, which is defined by the Harrison's conditions given by <sup>10</sup>:

$$\delta \ll (Dt)^{1/2} < \phi/2 \quad (3)$$

where  $\delta$  is the grain-boundary width,  $D$  is the volume diffusion coefficient and  $\phi$  is the grain size.

For B-type intergranular diffusion, it is not possible to measure directly the grain-boundary diffusion coefficient. However, Le Claire<sup>11</sup> has shown that it is possible to determine the product  $D'\delta$ , where  $D'$  is the grain-boundary diffusion coefficient, through the following relationship:

$$D'\delta = 0.661 \left( -\frac{\partial(\ln C)}{\partial x^{6/5}} \right)^{-5/3} \left( \frac{4D}{t} \right)^{1/2} \quad (4)$$

In Eq. 4,  $D$  is the volume diffusion coefficient,  $t$  is the diffusion time, and the gradient  $\partial(\ln C)/\partial x^{6/5}$  is calculated from the tail of the diffusion profile in a plot of  $\ln C$  versus  $x^{6/5}$ , as shown in Fig. 4, for oxygen diffusion at  $900\text{ }^\circ\text{C}$ . Equation 4 is valid if the parameter  $\beta$ , defined by:

$$\beta = \frac{D'}{D} \frac{\delta/2}{(Dt)^{1/2}}$$

is greater than ten.

The experimental conditions and the results obtained for oxygen grain-boundary diffusion coefficients in pure and doped ZnO are listed in Table 1. The values of  $D$  used in Eq. 4 are those previously determined in item 3.1.

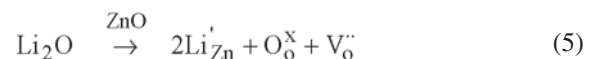
Figure 5 shows a comparison of the grain-boundary diffusion coefficients measured in doped and pure ZnO. Such as observed for the volume diffusion, in pure and Li-doped ZnO the grain boundary diffusion is not different, while in Al-doped ZnO the grain-boundary diffusion is greater than in pure ZnO.

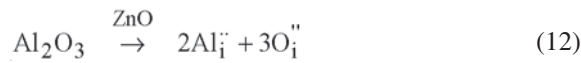
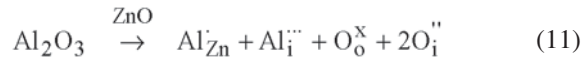
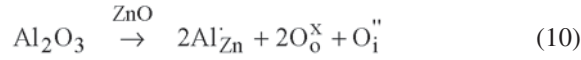
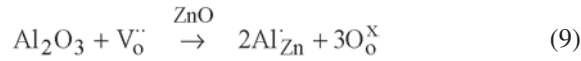
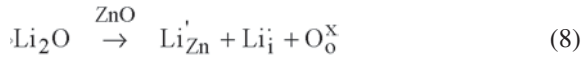
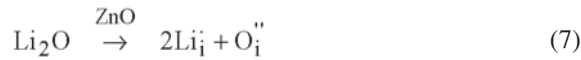
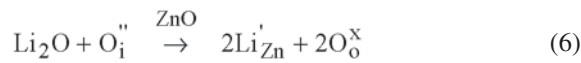
Assuming for  $\delta$  a typical value<sup>12</sup> of 1 nm, it is shown in Table 1, that the oxygen grain-boundary diffusion ( $D'$ ) is between three and four orders of magnitude greater than the volume diffusion ( $D$ ), in the same experimental conditions. These results show that grain-boundaries are fast ways for the oxygen diffusion in polycrystalline zinc oxide.

### 3.3 Diffusion mechanism

According to Figs. 3 and 5, oxygen diffusion in pure and Li-doped ZnO is similar, whilst the oxygen diffusion in Al-doped ZnO is greater than in pure ZnO.

In order to explain these results, equations describing the incorporation of Li and Al into ZnO structure must be written. These equations will be written using Kröger and Vink's notation<sup>13</sup>, and assuming the different possibilities of incorporation of the impurities in the ZnO structure, i.e., the cation impurities may occupy a regular site of the  $\text{Zn}^{2+}$ , or an interstitial site, or still both positions simultaneously, as follows:





Equations 5-8 describe the possible ways of incorporation of Li in ZnO structure, while Eqs. 9-12 describe the incorporation of Al.

We will begin the discussion assuming for the oxygen diffusion a vacancy mechanism. If the vacancy is a doubly charged vacancy ( $\text{V}_o''$ ), then the diffusion coefficient must be proportional to the  $\text{V}_o''$  concentration, i.e.,  $D \propto [\text{V}_o'']$ .

In pure ZnO, as used in this work, the vacancy is an intrinsic point defect and should be formed by the Schottky disorder given by:



If the vacancy concentration is changed, the diffusion coefficient should change too. Equation 5 shows that the incorporation of Li increases the vacancy concentration,

**Table 1.** Oxygen diffusion in pure and doped ZnO

Material	T (°C)	t (s)	D (cm <sup>2</sup> /s)	D'δ (cm <sup>3</sup> /s)	D'/D	β
ZnO	900	1.764 × 10 <sup>5</sup>	5.53 × 10 <sup>-17</sup>	2.37 × 10 <sup>-20</sup>	4.30 × 10 <sup>3</sup>	68.8
ZnO	950	8.430 × 10 <sup>4</sup>	1.23 × 10 <sup>-16</sup>	6.706 × 10 <sup>-20</sup>	5.45 × 10 <sup>3</sup>	84.6
ZnO	1000	3.060 × 10 <sup>4</sup>	1.13 × 10 <sup>-15</sup>	8.63 × 10 <sup>-19</sup>	7.64 × 10 <sup>3</sup>	65.1
ZnO-Al	900	1.764 × 10 <sup>5</sup>	8.97 × 10 <sup>-16</sup>	2.70 × 10 <sup>-19</sup>	3.00 × 10 <sup>3</sup>	11.9
ZnO-Al	1000	3.060 × 10 <sup>4</sup>	4.30 × 10 <sup>-14</sup>	2.64 × 10 <sup>-17</sup>	6.13 × 10 <sup>3</sup>	16.9
ZnO-Li	900	1.764 × 10 <sup>5</sup>	5.40 × 10 <sup>-17</sup>	2.2 × 10 <sup>-19</sup>	4.07 × 10 <sup>3</sup>	66.0
ZnO-Li	1000	3.060 × 10 <sup>4</sup>	9.46 × 10 <sup>-16</sup>	1.09 × 10 <sup>-18</sup>	1.14 × 10 <sup>3</sup>	105.9

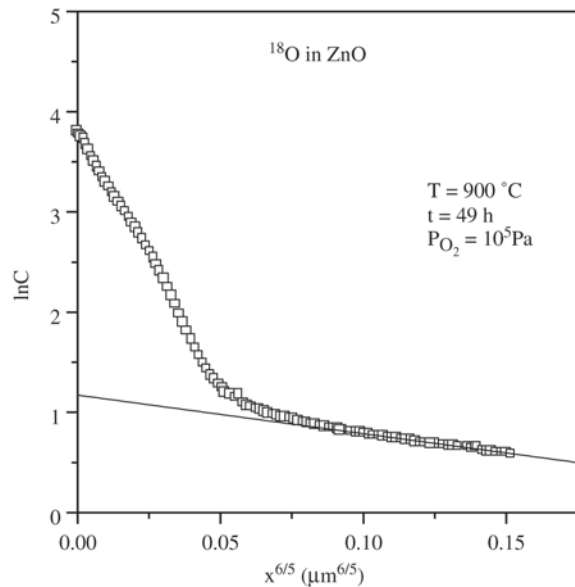


**Figure 4.** Oxygen concentration plot against  $x^{6/5}$  for oxygen diffusion in pure ZnO (900 °C, oxygen pressure 10<sup>5</sup> Pa, 1.764 × 10<sup>5</sup> s).

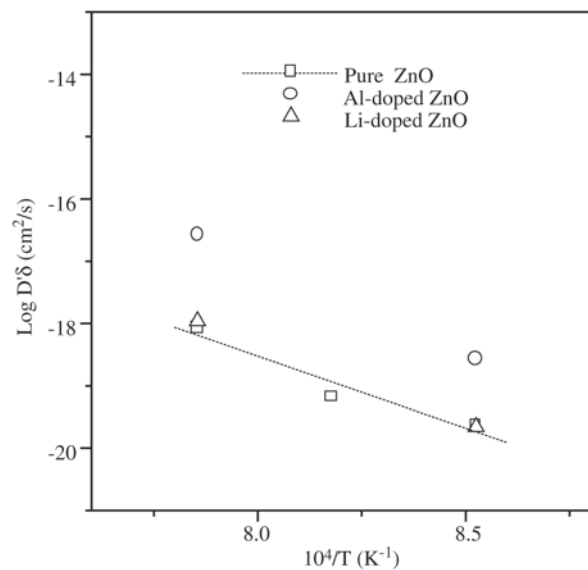


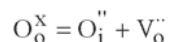
**Figure 5.** Comparison of the oxygen grain-boundary diffusion coefficients determined in pure and doped ZnO.

which should enhance the oxygen diffusion. This was not observed in Li-doped ZnO, in which the oxygen diffusion is similar to that in pure ZnO.

On the other hand, Eq. 9 shows that the incorporation of Al decreases the vacancy concentration. This should decrease the diffusion coefficient, which is not supported by the diffusion experiments, which show an enhancement of the oxygen diffusion in Al-doped ZnO.

So, the experimental results for oxygen diffusion in pure and doped ZnO are not compatible with a vacancy mechanism for oxygen diffusion in ZnO.

Let's assume now an interstitial mechanism for oxygen diffusion. In this case, the diffusion coefficient should be proportional to the interstitial oxygen, i.e.,  $D \propto [O_i^{''}]$ . In pure ZnO, doubly charged interstitial oxygen ( $O_i^{''}$ ) is an intrinsic point defect formed by the Frenkel disorder in the oxygen sublattice as follows:



Equation 6 shows that the incorporation of Li into ZnO decreases the concentration of interstitial oxygen, while Eq. 7 shows an increase of the interstitial oxygen concentration. Both cases, described by Eqs. 6 and 7, should affect the diffusion coefficient in Li-doped ZnO in regard with that in pure ZnO, for an interstitial mechanism. However, both cases do not agree with the diffusion experiments, in which the oxygen diffusion in Li-doped ZnO is similar to that in pure ZnO.

So, Eq. 8 should describe the incorporation of Li into ZnO, in the experimental conditions used, because, in this case, there is no change of the oxygen intrinsic point defects, and, consequently, no change of the oxygen diffusivity.

Equations 10-12 show different possibilities of incorporation of Al into ZnO with the formation of interstitial oxygen. So, the oxygen diffusion enhancement in Al-doped ZnO appears to be related to the increase of the interstitial oxygen concentration, which suggest an interstitial mechanism for oxygen diffusion in ZnO. In such case, the incorporation of the Al should be described by one of the Eqs. 10-12.

The behaviour observed for the oxygen grain-boundary diffusion in pure and doped ZnO is similar to that observed for the volume diffusion, i.e., no influence of Li, and enhancement of the diffusion in Al-doped samples. It suggests that the oxygen diffusion in ZnO grain-boundaries takes place by means of a mechanism similar to that of volume diffusion.

In a previous work, Haneda et co-workers<sup>7</sup> observed that in Li-doped ZnO the oxygen volume diffusion coefficients were lower than in pure ZnO, and in Al-doped ZnO the oxygen diffusion coefficients were greater than in pure ZnO. These results of Haneda *et al.*<sup>7</sup> are also consistent with an

interstitial mechanism for oxygen diffusion in ZnO.

In spite of that difference concerning the oxygen diffusion in Li-doped ZnO, the present work and that of Haneda *et al.* have found no experimental evidence for oxygen diffusion in ZnO by means of a vacancy mechanism, and clearly show that oxygen diffusion in ZnO takes place by means of an interstitial mechanism.

#### 4. Conclusions

- Oxygen diffusion coefficients were determined in pure and doped zinc oxide with the aim to identify the oxygen diffusion mechanism.
- Between 900 and 1000 °C, under a oxygen pressure of  $10^5$  Pa, oxygen diffusion in ZnO grain-boundaries is ca. 3 to 4 orders of magnitude greater than volume diffusion, in the same experimental conditions. Hence the grain-boundary provides a fast path for oxygen diffusion in ZnO.
- In our experimental conditions, oxygen volume diffusion in Li-doped ZnO is similar to the oxygen volume diffusion in pure ZnO, but oxygen volume diffusion in Al-doped ZnO is greater than oxygen volume diffusion in pure ZnO. These observations are also valid for the oxygen grain-boundary diffusion in pure ZnO, in Li-doped ZnO and in Al-doped ZnO. These results suggest an interstitial mechanism for oxygen diffusion in ZnO.

#### Acknowledgements

This work was supported by Fundação de Amparo à Pesquisa do Estado de Minas Gerais (FAPEMIG), Brazil.

#### References

1. Gupta, T.K.; Carlson, W.G. A Grain-Boundary Defect Model for Instability/Stability of a ZnO Varistor. *J. Mater. Sci.*, v. 20, p. 3487-3500, 1985.
2. Gupta, T.K. Applications of Zinc Oxide Varistors, *J. Am. Ceram. Soc.*, v. 73, n 7, p. 1817-1840, 1990.
3. Moore, W.J.; William, E.L. Diffusion of Zinc and Oxygen in Zinc Oxide, p. 89-93. In: Crystal Imperfections and the Chemical reactivity of Solids. *The Faraday Society*. Aberdeen, Scotland, p. 86-93, 1959.
4. Hoffman J.W.; Lauder, I. Diffusion of Oxygen in Single Crystal Zinc Oxide. *Trans. Faraday Soc.*, v. 66, p. 2346-2353, 1970.
5. Robin, R.; Cooper, A.R.; Heuer, A.H. Applications of nondestructive single-spectrum proton activation technique to study oxygen diffusion in zinc oxide. *J. App. Phys.*, v.44, n 8, p. 3770-3777, 1973.
6. Hallwig, D. PhD Dissertation, University of Erlangen, Nürnberg, Erlangen, Germany, 1979.

7. Haneda, H.; Sakaguchi, I.; Watanabe A.; Tanaka, J. *Defect and Diffusion Forum*, v. 143-147, p.1919-1224, 1997.
8. Tomlins, G.W.; Routbort J.L.; Mason, T.O. *J. Am. Ceram. Soc.*, v. 81, n. 4, p. 869-876, 1998.
9. Philibert, J. *Atom Movements, Diffusion and Mass Transport in Solids. Les Editions de Physique. Les Ulis. France. 1991*
10. Harrison, L.G. *Trans. Faraday Soc.*, v. 57, p. 1191, 1961.
11. Le Claire, A.D.; *Brit. J. Appl. Phys.*, v. 14, p. 351, 1963.
12. Atkinson, A.; Taylor, R.I. *Phil. Mag. A*, v. 43, p. 979, 1981.
13. Kröger, F.A. *The Chemistry of Imperfect Crystals. North-Holland Publishing Co., Amsterdam, Netherlands, 1974.*